Swelling and Erosion Affecting Flavor Release from Glassy Particles in Water

P. E. Bouquerand, S. Maio, and V. Normand
Firmenich S.A., 1217 Meyrin 2 Geneva, Switzerland

S. Singleton and D. Atkins
Unilever Colworth, Colworth House, Sharnbrook Beds, MK44 1LQ, U. K.

DOI 10.1002/aic.10267
Published online in Wiley InterScience (www.interscience.wiley.com).

A model of flavor release from encapsulated flavor particles immersed in water has been developed that correlates well with experimental data. Flavor release from particles was determined by measuring both the quantities released from the particle to water and from water to air in the headspace. The model presented here predicts a very different release with time from the encapsulated flavor if the particle develops a hydrogel at the surface (swelling) compared to gradual erosion. Controlled heating showed more retention of flavor when the particle swells compared to a more rapid flavor release under conditions of particle erosion. © 2004 American Institute of Chemical Engineers *AIChE J,* 50: 3257–3270, 2004

Keywords: encapsulated flavor, mass transfer, erosion, swelling, water-diffusion coefficient

Introduction

Most of the key flavor components are volatile and are by definition the most difficult to retain because they are the first molecular species to escape. In savory products, for example, the loss of volatile molecules is crucial for the flavor impact. Furthermore, a number of cooking processes (such as instant soups, dough, broth cube) often involve dispersion of flavor components in an excess of hot water, which then volatilize too quickly.

A method for protecting flavors from adverse conditions during storage, and therefore enhancing the shelf life of flavor, is to confine the volatile molecules in a glassy matrix (Benczédi, 2002; Schultz et al., 1955). This is achievable if the storage temperature is lower than (Benczédi and Bouquerand, 2001) or close enough to the glass-transition temperature (T_g) (Blake and Attwool, 1998) and if the relative humidity is low enough to ensure stability of the glass. Under these conditions, the volatiles inside the particles are trapped in the solid glassy structure. When these particles are exposed to temperatures higher than the T_g, the glassy matrix goes through a second-order transition. As a result, it becomes rubbery; the mobility of the volatiles increases and the flavor leaves the particle. The T_g of a water-soluble matrix also decreases with uptake of water from the surrounding environment. As they soften, particles can either dissolve or swell. Depending on the application, it is sometimes desirable to have different release kinetics: quick (such as instant beverages) or slow (such as instant soups or food that needs to be cooked before consumption).

Most flavor-encapsulated particles are based on starch hydrolysate (maltodextrin) matrices, which are known to deliver rapidly in wet conditions (Mutka et al., 2000). For some applications that need cooking, a slower release is preferred, to minimize losses during preparation up to the time of consumption. This is achievable when an external hydrophobic barrier protects the particle from dissolving too quickly (that is, coating) or if the particle integrity is preserved for longer times (that is, swelling, which is the subject of the present work) (McIver et al., 2002).

Our aim in this report is to consider both the quick and slow

Correspondence concerning this article should be addressed to P. E. Bouquerand at pierre.bouquerand@firmenich.com.

delivery systems using models based on the self-diffusion of water.

Within an individual particle, various processes can occur when it is immersed in water, depending on the temperature of the water and the composition of the flavor carrier matrix. In this work, the water uptake that induces swelling or erosion of the particles will be considered as the diffusive process that drives flavor release.

Many models have been published dealing with the erosion-controlled release or swelling-controlled release, but these have been mainly concerned with drug delivery systems (nonvolatile molecules) (for reviews, see Fan and Singh, 1989; Narasimhan and Peppas, 1997). Both approaches are logically used in the appropriate cases; however, a general model that can describe both phenomena would provide an elegant solution to the problem.

The model developed here is based on a single particle that can either dissolve or swell, depending on slight changes in the composition of its supporting matrix, and can explain the time–intensity profile of flavor release to water and to the air. This model was adapted from the extensive work carried out on rice cooking (Davey et al., 2002; Suzuki et al., 1976, 1977) and the behavior of wheat grains in hot and wet conditions (Landman and Please, 1999; Stapley et al., 1998).

(1) A model for flavor release to air was developed based on the kinetic effect of water on glassy particles.

(2) NMR and microscopy measurements were used to define the necessary physical parameters characterizing the effect of water on the glassy particles.

(3) Flavor release from particle to water and from water to air was tested against the model using UV measurement and real-time headspace analysis, respectively.

(4) Implications of the theoretical model are demonstrated by heating the particles under controlled conditions, to illustrate what would happen, say, during cooking of an instant soup.

Experimental

Fabrication of flavored particles

Two types of particle were used in this study. A classic particle (particle A) produced according to Benczédi and Bouquerand (2001) and a newly designed particle, with swelling rather than dissolution behavior (particle B), produced according to McIver et al. (2002). Maltodextrin 10DE (Roquette, Lestrem F-62) forms the supporting matrix for both types of particle (59.73% w/w for particle A and 57.39% w/w for particle B). The flavor encapsulated is "Chicken 700611.05PI" (Firmenich S.A., Geneva, CH-1217) and represents 32.17% w/w of particle A and 30.21% w/w of particle B. The hydrogel precursor (HPG) used in this study is agar–agar (Sigma-Aldrich Chemie, Steinheim, Germany), which represents 3.3% w/w of the composition of particle B.

The water content of particles has been measured using the Karl–Fischer method and was 8.10% w/w for particle A and 8.40% w/w for particle B. Values of the glass-transition temperature (T_g) for particles A and B, measured by differential scanning calorimetry, were 44 ± 1 and 42 ± 1°C, respectively. The concentration of dimethyl sulfide was 0.03% w/w and the concentration of eugenol (4-allyl-2-methoxyphenol) was 9.7×10^{-3}% w/w in both samples.

NMR

The self-diffusion of water in the particle as a function of the water-phase volume was measured using pulsed-field gradient NMR. The particles used for these measurements were unflavored and uncolored, but had similar T_g values (39.5 ± 1°C) and maltodextrin species and origin. The water content of the dry particles was 9.57% w/w measured by the Karl–Fischer technique. The NMR samples were prepared directly in 10 mm O/D NMR tubes. Each sample was prepared such that its final volume was about 1 mL. This was achieved by initially weighing in the required amount of particles, followed by weighing in the required amount of water. The samples were then left for at least 2 days to allow dissolution of the particles in the water, followed by careful stirring, to ensure uniform mixing before any NMR measurement. The initial moisture content of the particles was included in the final water content determination for each sample prepared.

The self-diffusion coefficients of the water in the samples were measured at temperatures of 25, 40, and 60°C using a Resonance Instruments (Witney, UK) MARAN Ultra 20 NMR spectrometer. Sample temperatures were controlled to within ±1°C using the standard MARAN gas flow temperature control system, and these were calibrated using a thermocouple for each temperature studied. The self-diffusion coefficients were measured using the pulsed magnetic field gradient stimulated echo-pulse sequence (Tanner and Stejskal, 1968). A magnetic field gradient of 2.13 T m^{-1} with 10-ms time between the gradient pulses was used for all samples > 30% w/w moisture content. A higher magnetic field gradient of 3.14 T m^{-1}, with a shorter time of 5 ms between the gradient pulses, was used for the samples with water content < 30% w/w. The echo attenuation was recorded as a function of increasing pulse width of the gradient pulses for each sample, and the results were fitted according to Tanner's relationship (Tanner and Stejskal, 1968) using standard Resonance Instruments software (RI Diffusion). The magnetic field gradients were initially calibrated by measuring the echo attenuation as a function of increasing gradient pulse width for pure water at 25°C, and the gradient strengths were then calculated from the known self-diffusion coefficient of water at 25°C.

Microscopy measurements

Microscopy measurements were carried out using a Wild Makroskop 420 (Leica Microsystems, Milton Keynes, UK) with an approximate magnification of ×30 on the image monitor. A microscope temperature-controlled stage was used at preset temperatures (Leitz Heating Stage 80, Leica Microsystems). This enabled the characterization of single flavor particles in a glass petri dish filled with distilled water. The radius of the particles was determined from maximum surface projection measurements. Initial particle radii were 1.17 ± 0.05 and 1.35 ± 0.05 mm for particles A and B, respectively. Using image-analysis software (KS400, Imaging Associates, Thame, UK), it was possible to estimate the maximum surface area change of the particle immersed and therefore the radius considering spherical shapes. Images were acquired with a time frequency of 2 s for analysis.

Spectroscopy measurements

The flavor composition was complex and was formed by the combination of 62 different molecular species. Fortunately, the flavor absorbs in the UV, showing a peak proportional to its concentration in water at 255 nm, which corresponds to benzenyl properties. Maltodextrins and HGP do not absorb significantly at this wavelength. In this work, the molecules or group of molecules that absorb light at this wavelength are called "tracers" for simplification and are treated as one compound according to the additivity rule of optical density. This is dependent on the sample's being homogeneous before immersion. The absorption measurements were carried out using a Perkin–Elmer Lambda 25 spectroscope, coupled to a hermetic dissolution cell (Erweka DT700) filled with water (volume 1000 cm^3, mass of particle 2.50 g, and temperature 40°C). The liquid was continuously cycled from the dissolution cell to the measurement cell (standard quartz cuvette with 1-cm optic path; flow rate: 17 cm^3/min). The measurement of the variation in absorbance was performed in real time.

Headspace

Headspace measurements were carried out using a 613-cm^3 bottle linked to an atmospheric pressure chemical ionization mass spectrometer (APCI-MS) (Linforth et al., 1996). The volume of water used was 50 cm^3 for a mass of 0.5 g of particles. The bottle was maintained at a constant temperature using a water bath. The contents of the bottle were continuously stirred at 60 rpm using a magnetic stirrer. Several volatile species contained in the particles were measured and analyzed in real time using the APCI-MS. A continuous and constant airflow (30 $cm^3\ min^{-1}$) carried a volume of air from the bottle to the MS. For low volatile concentration in the air, the amplitude of the signal could be substantially affected by the disappearance of the molecules measured. Once equilibrium had been reached, the disappearance of a volatile, attributed to the washout of vapor molecules into the MS, was characterized by a slight and linear decrease in the intensity with time. Therefore, the apparent intensity was corrected by subtracting the negative slope throughout the time scale to give the true intensity profile of the volatile species considered. Given that the amplitude of the MS signal was proportional to the number of molecules ionized, it followed that the MS signal measured the variation in concentration of flavor molecules at constant flow rate.

The controlled heating experiment was carried out under the same experimental conditions as previously described (that are, bottle volume, water quantity, temperature, and stirring rate). However, MS measurements were preceded by a 15-min particle immersion in water under $6 \times 10^3\ cm^3\ min^{-1}$ nitrogen flow in open conditions, thus ensuring the renewal of the headspace.

Among the volatile molecules measured it was pertinent to follow the release of dimethyl sulfide (C_2H_6S) because it is very volatile (vapor pressure 10,420 Pa at 20°C), hydrophobic ($\log P = 0.86$ at 20°C, where P is the octanol/water partition coefficient), and small ($M_w = 62.13\ g\ mol^{-1}$). This molecule is commonly found in cheese and cooked meat. Because of its high volatility, it is also a good tracer for the flavor release. The eugenol is a heavier molecule ($M_w = 164.20\ g\ mol^{-1}$), more hydrophobic ($\log P = 2.41$ at 20°C), and less volatile (vapor pressure 1.77 Pa at 20°C).

Theoretical Development

Several assumptions are necessary in defining the model for flavor release:

- Low molecular weight volatiles, which constitute the most difficult compounds of a flavor to trap, are homogeneously distributed within the dry particle.
- The mobility of these molecules is identical in the hydrated particles to what it would be in water (Siepmann et al., 1999) because the volume occupied by the molecule is small compared to the hydrogel mesh size. Therefore, it was assumed that no interactions exist between the volatile and the hydrogel network, as suggested elsewhere (Lopes Da Silva et al., 2002).
- The aqueous medium is homogeneous at all times when the solution is constantly stirred.
- No chemical interaction exists between the flavor molecules and the matrix material of the particle.

Flavor release from particle to water

Based on these assumptions, together with the understanding that the tracer molecule is able to migrate out of the particle, two different mechanisms are conceivable.

(1) The polymer is totally solvated and migrates into the solution (Parker et al., 2000; Peppas et al., 1994).

(2) The polymer molecule responsible for the hydrogel formation partially detaches from the glassy core and restructures itself before total separation can occur. If hydration increases the flexibility of the polymer molecule, a network permeable to small molecules forms. The gel is still attached to the glassy matrix and resistant enough to ensure the integrity of the particle.

Davey et al. (2002) considered the swelling of a rice grain for dissolution purposes in beer production with the migration of a "gelatinization" front toward the center of the grain. For rice cooked in water, temperature is a critical parameter: rice grains swell at low temperature but at high temperature they dissolve. Here, at a given temperature, one composition of particle favors swelling, whereas a different composition promotes particle erosion.

Model for Swelling Particles. Water motion within glassy starch particles is driven by a chemical potential gradient. This gives rise to a Fickian diffusion mechanism for the water uptake. As the water is absorbed by the particle, the starch structure will swell or dissolve to accommodate the additional water. It has been suggested that rice grains take up water for hydrogel formation.

Using NMR, it has been proven that the waterfront in wheat grains moves approximately linearly with time in wet conditions (Stapley, 1995; Stapley et al., 1997). If this is true for natural particles such as whole-wheat grains (Landman, 1999) and for rice grains (Takeuchi et al., 1997a,b), this may also be expected for glassy maltodextrin particles.

As a consequence of the Fickian diffusion mechanism of water into the glass particle, the water self-diffusion in the glassy matrix depends on the water-phase volume. As the water content of the particle increases, its self-diffusion increases. Water self-diffusion has been measured as a function of mois-

ture content for wheat (Stapley, 1995), rice starch (Gomi et al., 1998), starch, and corn kernels (Syarief, 1984) using NMR. In all cases, the mobility of water increases "exponentially" as the water-phase volume increases. However, the self-diffusion coefficient evolution has been fitted by a variety of empirical functions with parameters explained by individually developed theories. In all cases, at high moisture content, it is found that using a simple exponential function of the moisture content gives a satisfactory fit (Peppas et al., 1994).

It has been shown that the self-diffusion of water inside a rice grain can be described using a nonlinear diffusion equation in spherical coordinates, implying diffusion of the solvent toward the center of the particle (Davey et al., 2002). This statement leads to the classical equation of mass conservation where $\phi(r, t)$ satisfies

$$\frac{\partial \phi}{\partial t} = \frac{\partial}{\partial r}\left[D(\phi)\, \frac{\partial \phi}{\partial r}\right] \tag{1}$$

where r is the radius of the spherical particle, ϕ is the phase volume of water, and $D(\phi)$ is the water self-diffusion evolution through the particle. It is common to transform each parameter to a dimensionless parameter because this eases the resolution and describes the phenomenon more than the effective results. This has the effect of generalizing the model to a wider range of materials

$$\frac{\partial \theta}{\partial \tau} = \frac{\partial}{\partial \rho}\left[\Delta(\theta)\, \frac{\partial \theta}{\partial \rho}\right] \tag{2}$$

The dimensionless parameters θ (phase volume), τ (time), ρ (radius), and the function $\Delta(\theta)$ (diffusion coefficient evolution with phase volume) are defined as

$$\theta = \frac{\phi - \phi_0}{\phi_1 - \phi_0} \qquad \tau = \frac{D(\phi_1)}{R_0^2}\, t$$

$$\rho = \frac{r}{R_0} \qquad \Delta(\theta) = \frac{D(\phi)}{D(\phi_1)} \tag{3}$$

where the water-phase volume ϕ_1 in the outer part of the swollen particle (from the outer boundary toward the waterfront) is constant; ϕ_0 is the initial water-phase volume in the dry particle; and R_0 is the initial dry particle radius.

A pertinent approximation to consider was the hypothesis of a pseudosteady state in the swollen region of the particle. As a consequence, Eq. 2 reduces to

$$\frac{\partial}{\partial \rho}\left[\Delta(\theta)\, \frac{\partial \theta}{\partial \rho}\right] = 0 \tag{4}$$

It is well known that the water mobility is an increasing function of the water-phase volume where the upper limit is the self-diffusion of water in water. As mentioned earlier, Gomi et al. (1998) showed that the water self-diffusion evolution at 25°C can be fitted by a sum of exponential functions of the water mass in rice grains. For simplicity, however, a single exponential function is also acceptable if the maximum phase volume of water is low enough before unity, but high enough to ensure no solvent quality effect on the flavor self-diffusion. Therefore

$$D(\phi) = D_0 \exp(k\phi)$$

$$\Delta(\theta) = \exp[k(\phi - \phi_1)] = \exp[k(\phi_1 - \phi_0)(\theta - 1)] \tag{5}$$

The function $\Gamma(\theta)$, a mathematical transform, is next defined as a tool for solving Eq. 4

$$\Gamma(\theta) = \int_0^\theta \Delta(\omega)\, d\omega = \frac{1}{k(\phi_1 - \phi_0)} \{\exp[k(\phi_1 - \phi_0)(\theta - 1)] - \exp[-k(\phi_1 - \phi_0)]\} \tag{6}$$

Here, it is assumed that the water-phase volume, from the center of the particle to the water diffusion front (ϕ_0), is constant and equal to the phase volume of the water in the particle before immersion. As a consequence, the system of equations determining the time evolution of the outer radius (r/R_0) and the inner waterfront (s/R_0) takes the following form where both radii can be redimensioned without loss of integrity

$$\begin{cases} \dfrac{dr}{d\tau} = \dfrac{\phi_1 - \phi_0}{1 - \phi_1}\, [\Gamma(1) - \Gamma(\theta_w)]\, \dfrac{1}{r^2\left(\dfrac{1}{s} - \dfrac{1}{r}\right)} \\ \dfrac{ds}{d\tau} = -\dfrac{\Gamma(1) - \Gamma(\theta_w)}{\theta_w}\, \dfrac{1}{s^2\left(\dfrac{1}{s} - \dfrac{1}{r}\right)} \end{cases} \tag{7}$$

The water-phase volume (ϕ_1) ahead of the incoming waterfront and toward the external boundary is set constant to ease resolution and, in reality, this is a sensible approximation. The phase volume at the waterfront (ϕ_w) is set constant. It physically corresponds to the phase volume of water necessary to unfold the gelling agent. Because the value of ϕ_1 is lower than unity, the water activity around the dry core of the particle is reduced.

Numerically solving this system of equations, and redimensioning the time, leads to the expressions of the volume of gel formed in the periphery of the particle (Eq. 8a). Equations 8b and 8c give the volume of wet maltodextrin and the mass of maltodextrin solvated, respectively (density of the starch d_s = 1.43 g cm^{-3})

$$V_{Gel}(t) = \frac{4}{3}\, \pi[r(t)^3 - s(t)^3] \tag{8a}$$

$$V_{wet}(t) = \frac{4}{3}\, \pi[R_0^3 - s(t)^3] \tag{8b}$$

$$m(t) = (1 - \phi_0) d_s V_{wet}(t) \tag{8c}$$

If the flavor molecules are considered as inert and homogeneously distributed in the maltodextrin-based glass and assuming that the glass is not perturbed by the presence of the

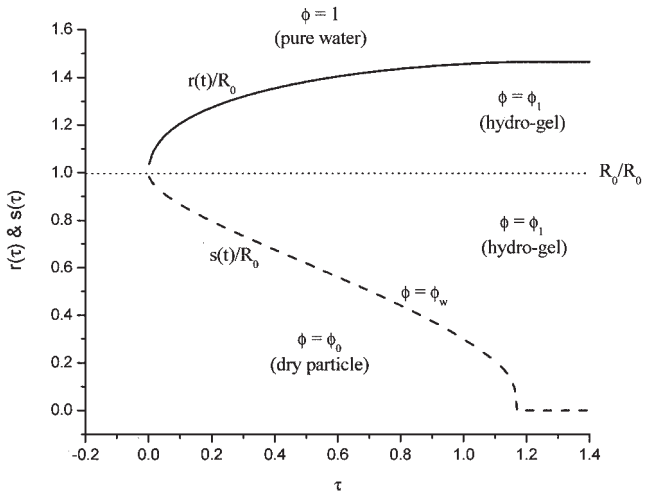

Figure 1. Evolution of the calculated swelling front and waterfront in the starch particle using ϕ_1 = 0.76, ϕ_w = 0.63, ϕ_0 = 0.116, and $D(\phi) = D_0 e^{k\phi}$.

volatile, the mass of flavor released in solution is directly proportional to the mass of polymer solvated, and is thus linearly related to $m(t)$ in Eq. 8c or $V_{wet}(t)$ in Eq. 8b.

Model for Erosion of Particles. An extension of the swelling behavior by water uptake is now considered for treatment of flavor release from a particle by erosion. In this case, the material lost by the particle depends on the ability of water to solvate the external layer of the polymer. The outer front progresses toward the center of the particle and effectively creates a membrane through which the polymer is released by reptation (Papanu et al., 1989). In the case of erosion, only the water penetration front is relevant for the calculation of tracer release, despite the fact that it is not easily measurable. In Davey et al. (2002) an adaptation of the swelling model is developed that uses a discrete calculation for both fronts. This model has been found more appropriate to particle A's behavior in water. The reason is that the particles studied in this work constitute low molecular weight starch hydrolysate molecules with high dextrose equivalent values compared to those of starch. Here, the linear backbone of the polymer is composed of only a few sugar units. This conformation does not allow much entanglement or gel formation, as suggested by the improvement of the dissolution process with a decrease in the molecular weight of the polymer (Devotta et al., 1994). The hypothesis that particles dissolve step by step, like peeling a shell of constant thickness, is made (Davey et al., 2002). In theory, once water has penetrated inside the particle for a distance δ, the wet external shell can separate from the core and solubilizes. This smaller particle core is then available for water uptake. Because the polysaccharide chain (starch derivative) is short, it is expected that δ is a very short distance.

In this last case, we assume the quantity of flavor molecules released in solution to be directly proportional to the volume of material, which separates from the particle.

To summarize the effect of water on particles, Figure 1 shows the evolution of the incoming waterfront (s) and the outer radius of the particle (r) in the case of swelling, corresponding to the resolution of Eq. 7 in dimensionless parameters.

Figure 1 presents four different phases. The origin of the graph is the location of the center of the particle at the time of immersion. At the origin of times, the dimensionless radius of the particle is 1.00 and above this dimensionless distance, the medium is simply pure water. As dimensionless time proceeds, water penetrates the particle following the dashed line toward the center of the particle with a waterfront phase volume ϕ_w. This corresponds to the water-phase volume necessary to unfold the gelling agent and to promote gelation. As a result of absorbing water, the particle swells and the external radius increases (solid line in Figure 1). The evolution of the external radius is therefore governed by the evolution of the wet front and experimental measurement of one of these two functions allows estimation of the other, providing that all needed parameters to solve Eq. 7 are accessible; that is, if the functions $r(t)$ and $D(\phi)$ are measured, only the fit of the tracer concentration release in water during immersion is necessary to access the phase volumes of water in the swelling phase of the particle (ϕ_1 and ϕ_w). From Eq. 8b, the concentration of flavor released into the surrounding liquid is available and, depending on whether the particle swells or erodes, different figures are obtained. These are presented in Figure 2.

When a particle erodes, water penetrates at a faster rate than if the particle swells (Davey et al., 2002).

Flavor release from water to air

In terms of flavor release, the objective is to consider the quantity released to the air from the flavor molecules released in the liquid (Marin et al., 2000).

If release to the headspace over a constantly stirred liquid is considered, and if a substantial volume of air is analyzed, the system undergoes a mass transfer "reaction." This is commonly written as Eq. 9, where the concentration difference is the driving force for the mass transfer. Flavor molecules are small compared to the mesh size of the swollen part of the particle. Therefore, a simple approximation that neglects the mass trans-

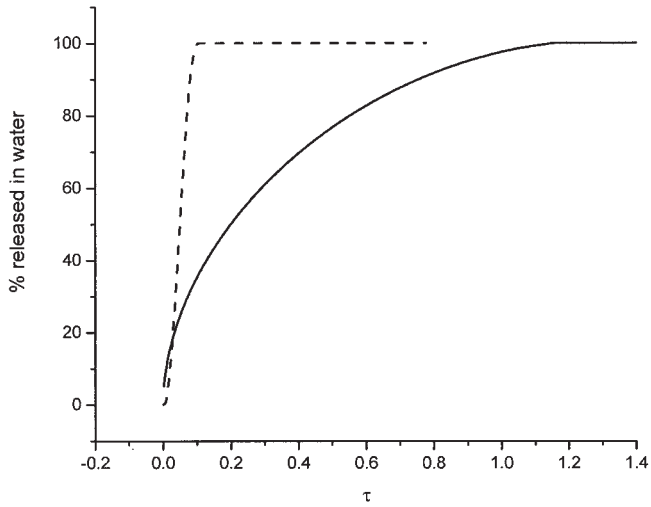

Figure 2. Estimated flavor concentration profiles in solution for erosion or swelling of starch.

All other parameters concerning the swelling are set at the same values than necessary for calculations shown in Figure 1.

port rate of volatile molecules from the hydrogel to the liquid is made. The volatile molecules equilibrate rapidly into the surrounding liquid following a dilution mechanism. This is true for small volatile molecules such as dimethyl sulfide and eugenol. Therefore, the mass transfer relationship responsible for the release to air concerns the actual transfer from the liquid to air

$$-\frac{dC_A}{dt} = \frac{k_{WA}S_{WA}}{V_{Air}}(C_A - K_{AW}C_W^*) \tag{9}$$

where subscripts A and W represent mean air and water, respectively; C is concentration; k_{WA} is the interfacial mass transfer constant rate and usually in the order of magnitude of 10^{-6} m s^{-1} (Coulson and Richardson, 1977); S_{WA} is the surface of the water/air interface available for the transfer; K_{AW} is the air/water partition coefficient (the asterisk represents the target equilibrium condition); V_{Air} is the volume of air over the solution. Equation 9 can be resolved analytically if the mass balance relationship is introduced with C_{p0}, the initial concentration of the flavor species considered in the dry particle, and C_W^* is determined (see Eq. 10). Therefore, at any time t, the following relationship is necessarily true

$$C_{p0}V_{wet} = C_W V_{Water} + C_W V_{Gel} + C_A V_{Air} \tag{10}$$

As the water progresses into the particle, the resolution becomes more complex and it is convenient here to assume a partial steady state at each measurement time. This takes the following form:

As time goes on, both the wet volume (V_{wet}) and the volume of the gel (V_{Gel}) evolve. From Eq. 10, it appears that the equilibrium conditions are defined as a function of time. Furthermore the next conditions characterize the equilibrium

$$C_{p0}V_{wet}(t=\infty) = C_W^*[V_{Water} + V_{Gel}(t=\infty)] + C_A^* V_{Air} \tag{11}$$

For any time t, the target equilibrium conditions are dependent on the water ingress. Therefore, a new mass balance relationship can be written where the equilibrium concentrations depend on time

$$C_{p0}V_{wet}(t) = C_W^*(t)[V_{Water} + V_{Gel}(t)] + C_A^*(t)V_{Air} \tag{12}$$

It is also important to consider that at the initial time of the immersion (t_0), concentrations in water and in air are zero. Then, the mass balance at equilibrium is (if the water uptake ceases)

$$C_{p0}V_{wet}(t_0+\delta t) = C_W^*(t_0+\delta t)[V_{Water} + V_{Gel}(t_0+\delta t)] + C_A^*(t_0+\delta t)V_{Air} \tag{13}$$

Then it is possible to approximate the number of molecules at equilibrium to the number of molecules effectively present in air

$$C_A^*(t_0+\delta t)V_{Air} \approx C_A(t_0+\delta t)V_{Air} \tag{14}$$

After substitution of Eq. 14 into Eq. 13 and rearranging, it becomes

$$C_W^*(t_0+\delta t) = \frac{C_{p0}V_{wet}(t_0+\delta t) - C_A(t_0+\delta t)V_{Air}}{V_{Water} + V_{Gel}(t_0+\delta t)} \tag{15}$$

Now, $V_{wet}(t)$ and $V_{Gel}(t)$ are functions that were determined earlier (see Eqs. 8a–8c) and cannot be part of the mass transfer between water and air phases (the particles dissolve or swell even if the air phase volume over the water is zero). In other words, flavor release does not affect the water ingress. Therefore, combining Eq. 15 and Eq. 9 and rearranging gives a differential equation characterizing the transfer, providing that δt is small (necessary condition for Eq. 14 to exist)

$$\frac{dC_A}{dt} = -\frac{k_{WA}S_{WA}}{V_A}\left\{C_A\left[1 + \frac{K_{AW}V_{Air}}{V_{Water} + V_{Gel}(t)}\right] - \frac{K_{AW}C_{p0}V_{wet}(t)}{V_{Water} + V_{Gel}(t)}\right\} \tag{16a}$$

Equation 16a can also be written in a simpler form as

$$\frac{dC_A}{dt} = -R[C_A P(t) - Q(t)] \tag{16b}$$

and Eq. 16 leads to

$$\int_{C_A(t)}^{C_A(t+\delta t)} \frac{dC_A}{C_A - \frac{Q(t)}{P(t)}} = -\int_t^{t+\delta t} P(t)\,R\,dt \tag{17}$$

Within a small time interval, $P(t)$ and $Q(t)$ can be considered as functions of time but independent of the kinetics involved here, and resolution of Eq. 17 according to Eq. 16b leads to the general equation

$$C_A(t+\delta t) = \left[C_A(t) - \frac{Q(t+\delta t)}{P(t+\delta t)}\right]\exp[-P(t+\delta t)R\delta t] + \frac{Q(t+\delta t)}{P(t+\delta t)} \tag{18}$$

Examples of simulated release for erosion and swelling of single particles are presented in Figures 3a and b.

Figure 3 shows the theoretical evolution of flavor concentration with dimensionless time. The simulation is made for a closed system involving 563 cm^3 of air on top of 50 cm^3 of water. The concentrations were calculated both in water (Figure 3a) and in air (Figure 3b) from a combination of Eq. 18 for the concentration in air and Eq. 10 for the concentration in water.

In both cases, the flavor is released from particle to water quicker than from water to the air. The signal in water increases rapidly, passes through a maximum, and then decreases because of the loss of volatile molecules to the air, toward an asymptotic signal value that corresponds to the equilibrium concentration in water. Simultaneously, the signal in air in-

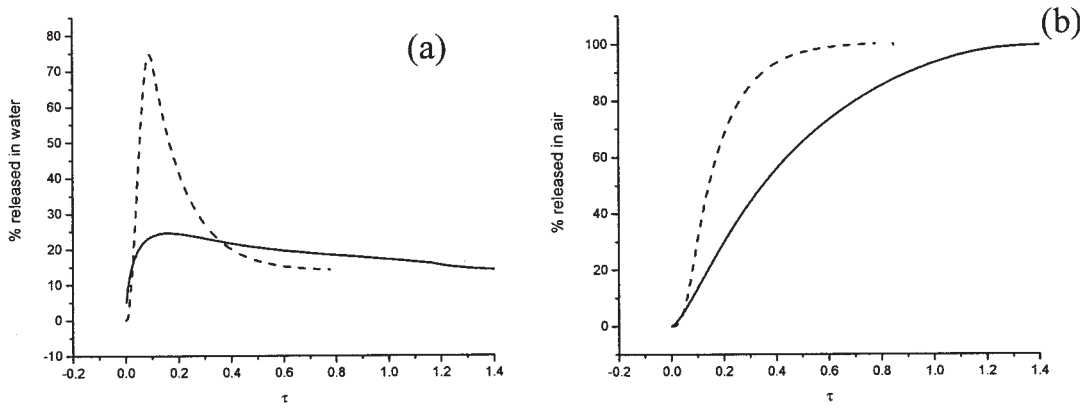

Figure 3. Simulation of flavor release in the water (a) and into the atmosphere over the water (b) when the particles are immersed.

The concentrations are expressed as relative to the equilibrium concentrations in a closed environment. The particles can either swell (solid lines) or erode (dashed lines). All other parameters are set at the same values than those necessary for calculations in Figures 1 and 2.

creases monotonically toward a value corresponding to the equilibrium concentration in air. Ultimately, the signal values at equilibrium (long time) are identical both in the liquid and in the air. Only the kinetics reveals the different behaviors, the release being slower when the particles swell.

Results and Discussion

NMR

Using NMR, the self-diffusion values of water in water, accurately measured at different temperatures of 25, 40, and 60°C, were 2.3, 3.22, and 4.69 $\times$ 10^{-5} cm^2 s^{-1}, respectively. The relationship between the diffusivity of water in the particle and the phase volume of water in the particle was determined for these three temperatures and results are shown in Figure 4 for a temperature of 40°C, relevant for the present study.

The fitting equation used was Eq. 6 and the parameters D_0 = 2.324 $\times$ 10^{-7} cm^2 s^{-1} and k = 4.275 were estimated using least-squares linear regression on a semilogarithmic scale for phase volumes greater than 50%. For a given starch molecule, D_0 is related to the temperature of the test, and increases when the temperature increases. The parameter k has been found to be independent of the temperature.

According to the literature, such a fit leads to parameter values such as D_0 = 1.62 $\times$ 10^{-7} cm^2 s^{-1} and k = 5.1 for rice grains with a satisfactory confidence (R^2 = 0.995) when using Gomi's data (Gomi et al., 1998). Similar values and water-phase–volume dependencies can be extrapolated from a different variety of whole-wheat grains. Examples for water self-diffusion coefficient in dry wheat grains range from 1.8 to 12 $\times$ 10^{-6} cm^2 s^{-1} for temperatures between 22 and 28°C (Callaghan et al., 1979; Eccles et al., 1988) and k ranges from 3.57 to 5.26 [from Stapley's data (Stapley et al., 1998)]. In evidence, k varies with the variety of the starch (such as rice, wheat, potato, etc.) and probably with the molecular weight and the degree of substitution of the polymer forming the continuous and protective glassy state. Full analyses of the relationship between water self-diffusion and water-phase volume would complete the understanding of the phenomenon.

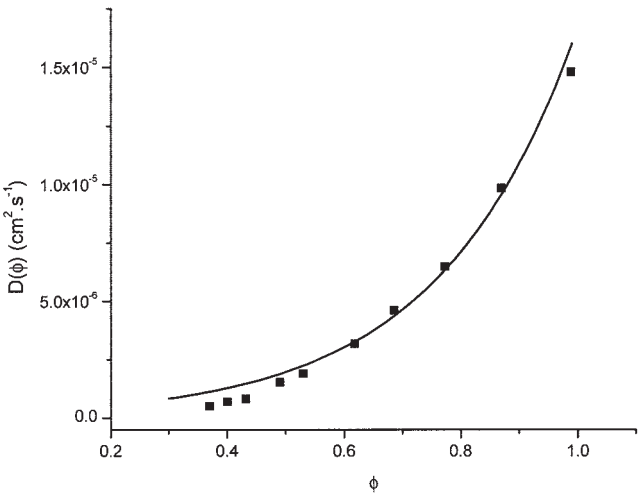

Figure 4. Evolution of $D(\phi)$ as a function of ϕ and fit using an exponential relationship for $\phi > 0.5$.

Microscopy image analysis

Using microscopy, it was possible to determine the evolution of the particle radius using image-analysis software. Figure 5 shows both the experimental data and the simulation from the resolution of Eq. 7 and according to the NMR results.

A representation of the same data obtained for short times (<20 min) is presented as an inset graph. The best fit of the model for experimental data of particle B has been found for ϕ_1 = 0.76 and ϕ_w = 0.63; ϕ_0 has been defined as the initial water volume fraction and estimated from the initial water weight fraction. According to the small quantity of HGP in particle B, it is assumed that the water-phase volume at the waterfront (ϕ_w) is identical for both particles A and B. Therefore, the best fit of the model to experimental data for particle A indicates that the difference between the water-phase volume at the waterfront and the water-phase volume where peeling occurs is only 10^{-4} (0.1% in volume). The depth of the layer before peeling is $\delta = 10^{-3}$ that, when redimensioned, gives a distance of 1.17 μm.

For both particle types, a deviation of the model to the

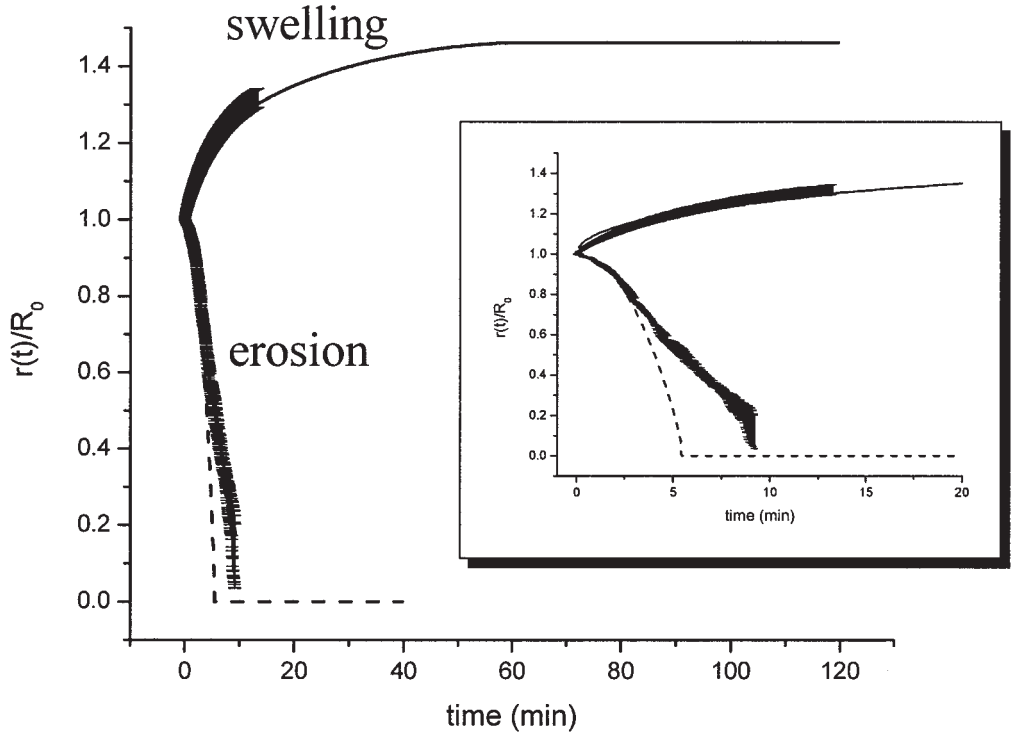

Figure 5. Evolution of the outer particle radius with time for two samples from microscopy investigation and fitting curve of *r*(*t*) according to Eq. 7.

The best fit was reached for $\phi_1 = 0.76$, $D_0 = 2.324 \times 10^{-7}$ cm^2 s^{-1}, and $k = 4.275$ for the swelling; calculations for erosion were plotted according to the same water diffusion function. Initial radii for particles A and B are 1.17 ± 0.05 and 1.35 ± 0.05 mm, respectively. For the erosion curve (dashed line), the depth of the layer before peeling is $\delta = 1.17 \times 10^{-3}$ mm with $\phi_1 - \phi_w = 10^{-4}$ and $\phi_w = 0.63$. Experimental data are plotted with standard deviations (bold curves) and calculated evolutions are the dashed line for erosion and solid line for swelling.

measurements is observed (see inset graph in Figure 5). However, for both categories of particles, this deviation can be discussed. For the swelling model, the particles are treated as perfect spheres and in reality the particles have a slightly pronounced oval shape. Nevertheless, a satisfactory agreement is obtained between the measurement and the model. For particles that erode, a good fit is obtained for the short times and a divergence appears after several minutes. This is directly related to the stirring rate of the solution, as demonstrated in Figure 6. According to Figure 4, if the polymer is not removed from the close neighborhood of the particle while this is eroding, the mobility of the water will be reduced outside the particle and the penetration rate will be affected. However, with the experimental conditions used, it was not possible to measure the particle shape while stirring.

The simple representation of the complete dissolution time against applied stirring rate is well fitted by the following equation

$$t_d = \frac{353.6}{\Omega} \tag{19}$$

where t_d is the time in minutes when total dissolution is observed and Ω is the stirring rate in rpm. A relationship that links the flux of material from the particle to the liquid as a function of the shear rate would have been more appropriated; however, it would have added unnecessary complexity to the demonstration. From Eq. 19, the dissolution of particle A can be achieved only if stirring is present. During the experiment, the agitation resulting from thermal convection corresponds roughly to a 40 rpm stirring under normal conditions. It is interesting to note that the beginning of the curve for particle A still fits well after 200 s when it can be suggested that the polymer released from the particle starts to substantially affect

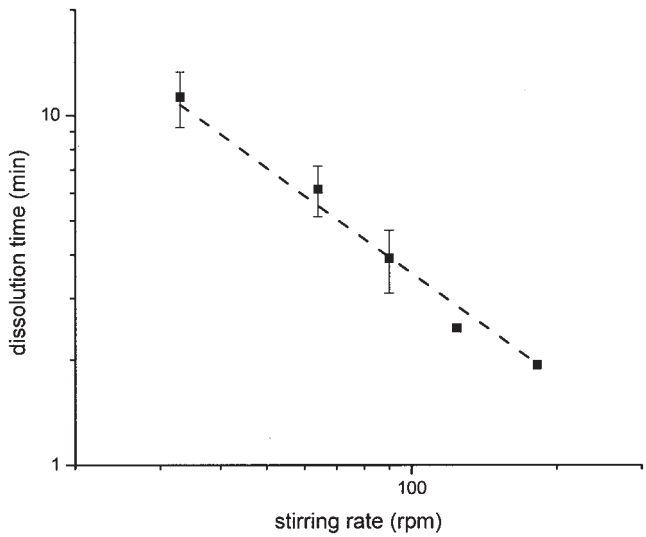

Figure 6. Influence of the stirring rate on the dissolution time for particle A at 40°C in distilled water.

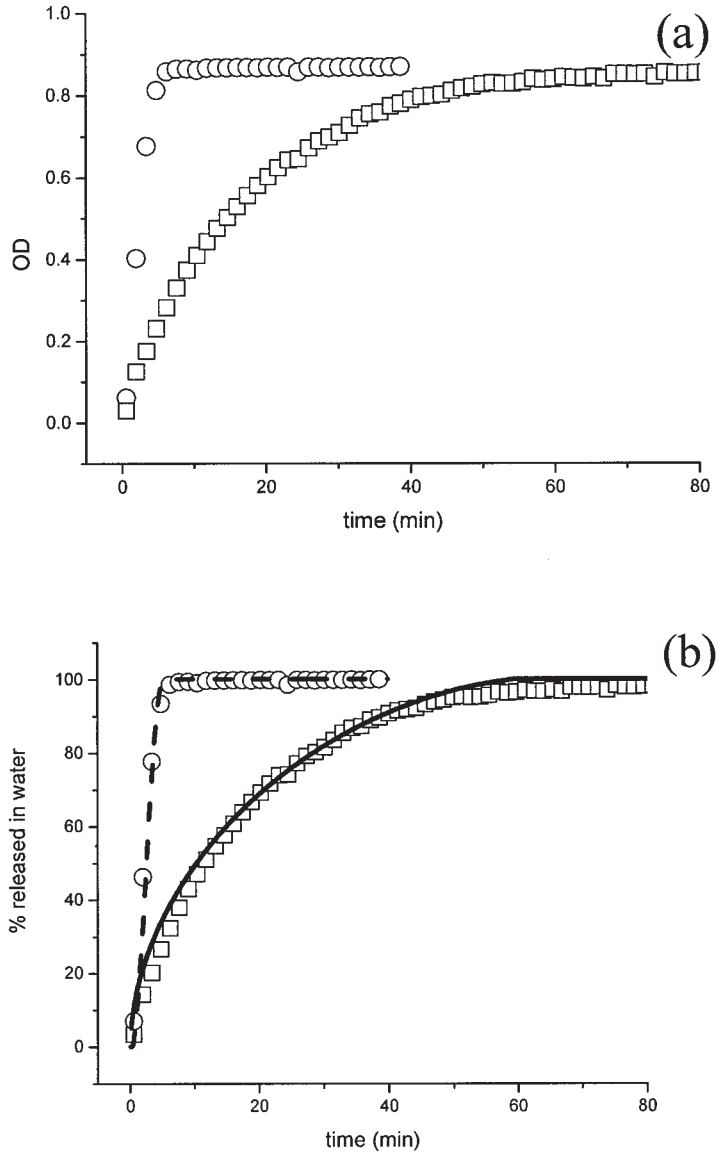

Figure 7. (a) Evolution of the concentration of flavor released in water from immersed particles measured by spectroscopy at 255 nm. Particle A: open circles and particle B: open squares. (b) Comparison of the experimental signal with the modeling for water uptake in real time considering the diffusion of water as a function of its phase volume.

Initial conditions: $V_A = 563$ cm^3, $S_{WA} = 47.8$ cm^2, $k_{WA} = 4 \times 10^{-5}$ ms^{-1}, $K_{AW} = 5.521 \times 10^{-1}$ (value at 40°C calculated using Eq. 21). Dashed lines for erosion and solid lines swelling.

the mobility of water outside. This would indicate that the first mechanism involved is limited by stirring.

UV and flavor flux

Kinetics spectroscopy measurements were performed at 255 nm. The Beer–Lambert relationship for the tracer intensity is linear until at least 9×10^{-4} g cm^{-3} of flavor with an R^2 value close to 0.997. The apparent constant of absorption for the flavor is $\varepsilon_{app} = 1.178 \times 10^{-3}$ cm^2 per gram of particle. The absorption of light at higher wavelength (results not shown) close to the infrared region does not increase significantly with the flavor concentration, showing that the solution's turbidity does not affect the measurement. Therefore, the optical density is proportional to the tracer concentration that is itself proportional to the level of flavor in solution. Spectroscopy measurements reveal the evolution of the tracer concentration in water, measured as a function of particle immersion time. Figure 7a shows that the maximum intensity obtained for both particles A and B at long times are identical. This indicates that the tracer concentration released in solution is roughly the same for both particle types. A rapid observation of optical density intensity as a function of t^n indicates that the tracer concentration evolves linearly with $t^{1.0}$ when released from particle A and linearly with $t^{0.5}$ when released from particle B. From this, both curves form a master curve before equilibrium (results not shown). This would indicate the erosion phenomenon to be

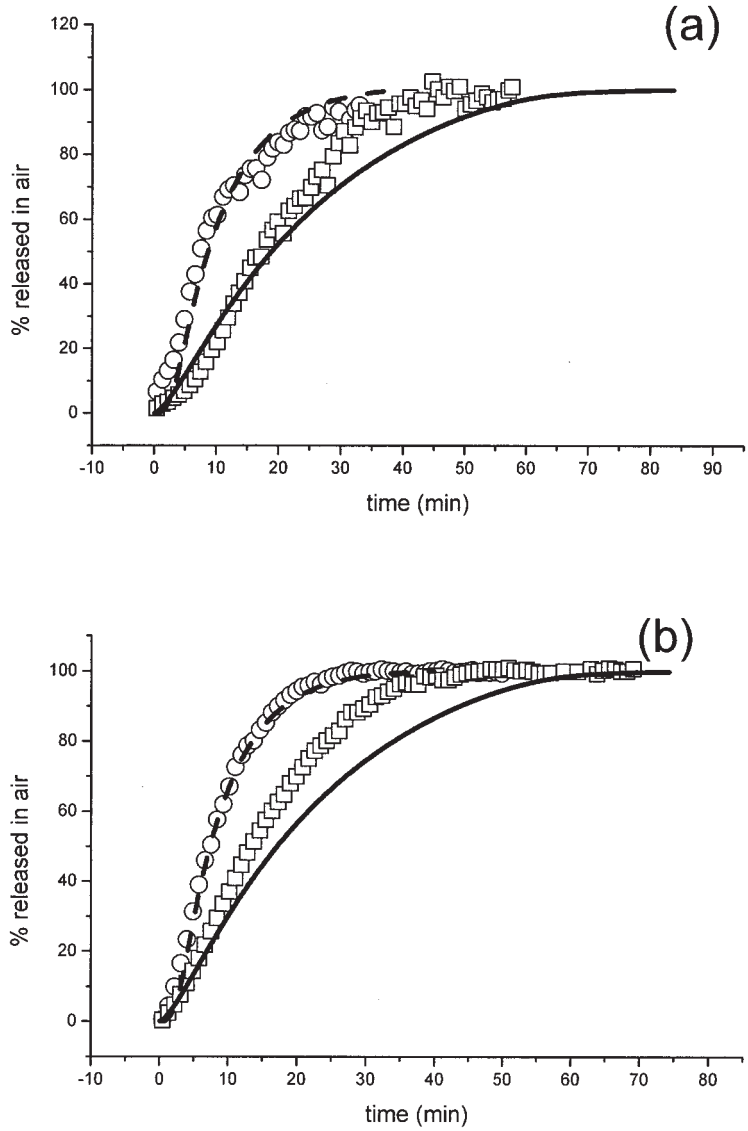

Figure 8. Comparison between experimental signal and modeling for (a) eugenol and (b) dimethyl sulfide appearance in air with time after immersion of particles A (open circles) and B (open squares) in 50 mL of water.

Measurements were carried out at 40°C using the same experimental conditions as used for the modeling (see captions for Figures 1–7). Dashed lines for erosion and solid lines swelling.

roughly a zero-order kinetics mechanism (Thomas and Windle, 1982) and the swelling behavior a purely classical Fickian diffusion mechanism.

The calculated intensity of the release (model) is considered as directly proportional to the wet particle volume $V_{wet}(t)$. The comparison between calculated (Eqs. 8b and 8c) and experimental values is presented in Figure 7b, where the percentage of release is considered (100% release corresponds to the maximum OD obtained for particle A at long times; dashed line in Figure 7a), and confirms the values of the parameters obtained from NMR and microscopy.

In the world of industry, it is common to evaluate the release performance of products in terms of flux. Because of the complexity of commercial products, a rough indication of the release rate is usually sufficient. The flux characterizing the release of material from the particle was calculated from the following equation to best fit the UV experimental data (Parker et al., 2000)

$$C_W(t) = C_0 \frac{4\pi R_0^3}{3V_{Water}} \left[1 - \left(1 - \frac{Jt}{\rho_0 R_0} \right)^3 \right]; \quad \frac{Jt}{\rho_0} \leq R_0 \quad (20)$$

where $C_W(t)$ is the concentration of the considered species released in the solvent and proportional to the optical density measured, C_0 is the initial concentration of that species in the glassy particle, and ρ_0 is the initial density of the particle. The only adjustable parameter for this cubic behavior is the mass flux (J). This has been estimated from the fit to experimental data presented in Figure 7 (results not shown) and is 2.35×10^{-2} and 0.31×10^{-2} g cm^{-2} s^{-1} for erosion and swelling, respectively. The formation of a continuous gel around the

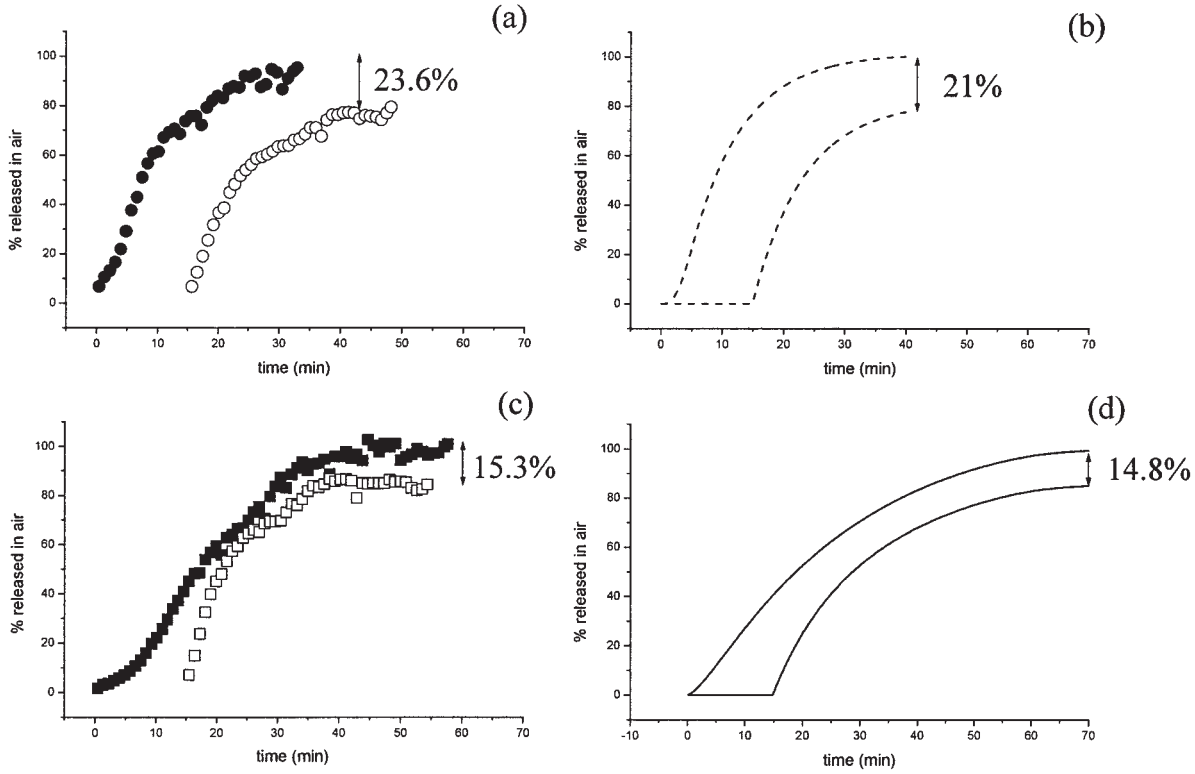

Figure 9. Eugenol: evidence of flavor retention by hydrogel formation under cooking situation, compared with data presented in Figure 8a.

(a) Experimental data for erosion (circles), (b) simulated data for erosion, (c) experimental data for swelling (squares), and (d) simulation for swelling (solid symbols: same experimental conditions as in Figure 8a and open symbols: same protocol but after 15 min of immersion in water at 40°C in open environment).

particle reduces the flux of matter roughly by a factor of 10 compared to erosion, but this is an indication of the performance of the two particles (A and B) upon immersion in water.

Headspace analysis

The quantity of flavor molecules in both particle A and particle B is thought to be initially identical. Therefore, once the carrier (particle) is dissolved or totally wetted, the amount of volatile molecules released in water is the same in the absence of an air phase (see Figure 7a). From this, the headspace signal at equilibrium (long time) must be identical. The headspace signal, proportional to the number of molecules of a given weight ionized, is expressed as a percentage of the intensity value obtained at long time where the signal is stabilized. The headspace intensity at a long time is the same for both particle types.

Headspace measurements corresponding to the release of eugenol and dimethyl sulfide and resulting from immersion of particle A and particle B in water are presented in Figures 8a and b, respectively.

The release difference between swelling and erosion of the particle is less obvious when the system equilibrates in the air compared to water (UV).

It has been recently demonstrated, using quantitative structure property relationships (Taylor and Linforth, 2001), that the air/water partition coefficient K_{AW} is strongly correlated to the log P value (octanol/water partition coefficient). This needs to be adjusted for changes in temperature. A rough, but useful, estimation of the water to air partition coefficient is approached by considering the following equation

$$K_{AW} \approx 2[T - T_{ref}]10^{-\log P - 1} \tag{21}$$

where T is the measurement temperature and T_{ref} is the temperature at which the log P is referred to. The advantage of estimating the partition coefficient is that it helps the determination of the flavor release in air. Only one adjustment parameter (k_{WA}) is now needed for the fit to one experimental results data set. Resolution of Eq. 18 for partition coefficient estimated by Eq. 21 is shown for eugenol and dimethyl sulfide in Figures 8a and b. In this exercise, the best accordance corresponds to where the rate constant k_{WA} equals 4×10^{-3} and 2×10^{-2} cm s^{-1} for dimethyl sulfide and eugenol, respectively. These values from now on are considered as constants for these molecules and will be used as such for the controlled heating experiment to simulate cooking.

Controlled heating experiment

Results from Figure 8 indicate that if the system is left in open conditions for a given time (lower than the time necessary for complete swelling of particle B), and then left closed until equilibration, particle B would release a higher quantity of flavor than particle A.

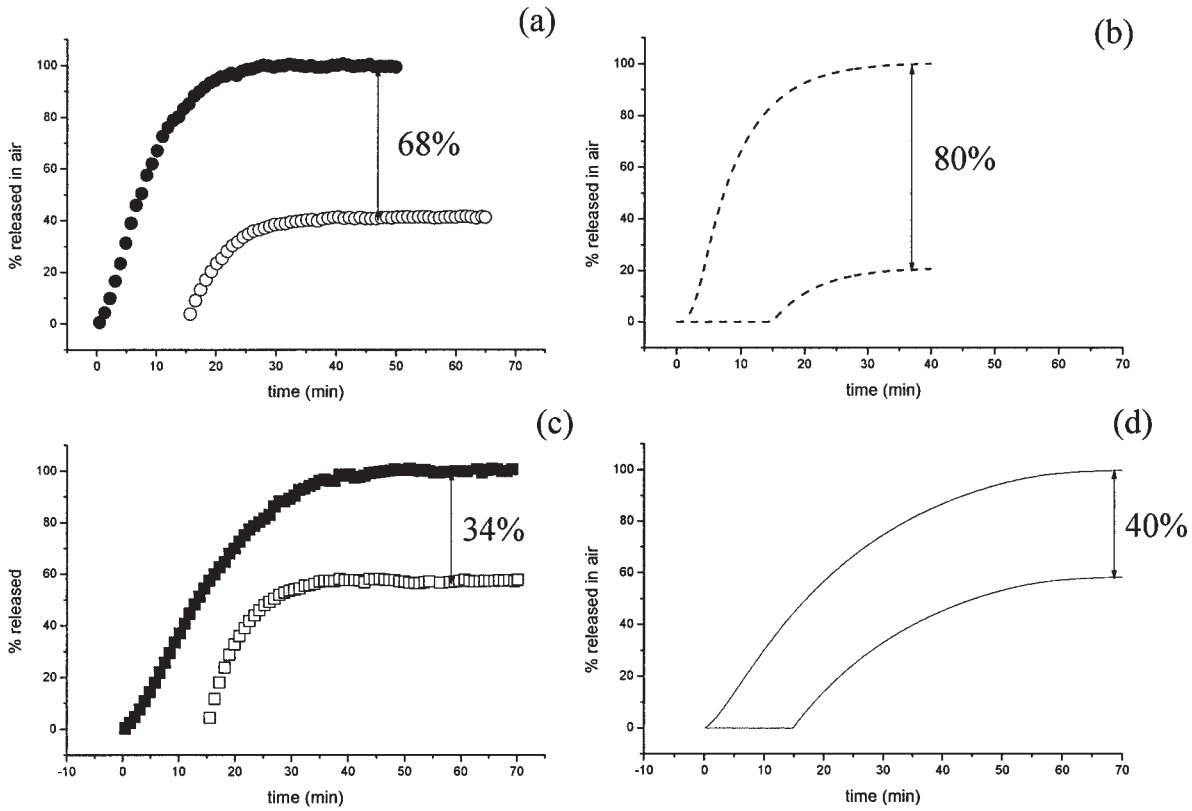

Figure 10. Dimethyl sulfide: evidence of flavor retention by hydrogel formation under cooking situation, compared with data presented in Figure 8b.

(a) Experimental data for erosion (circles), (b) simulated data for erosion, (c) experimental data for swelling (squares), and (d) simulation for swelling (solid symbols: same experimental conditions as in Figure 8a and open symbols: same protocol but after 15 min of immersion in water at 40°C in open environment).

The calculations corresponding to heating in an open environment for 15 min and then closed until equilibration are presented in Figures 9 and 10.

Here again, a good agreement is obtained between measurements and calculations for both molecular species. In a closed environment, the increase in flavor concentration in air is sigmoidal in shape. However, when the experiment was carried out in an open environment, the shape of the curve is exponential (Figures 9b and 9d and Figures 10b and 10d). At 40°C, particle B retains 85 ± 2% of eugenol (Figures 9a and 9b) and around 62 ± 5% of the dimethyl sulfide (Figures 10a and 10b) in the solution after 15 min of nitrogen flow. During erosion, only 76 ± 4% of eugenol (Figures 9c and 9d) and 41 ± 6% of dimethyl sulfide (Figures 10c and 10d) are retained. Considering this result, a change in the headspace concentration is expected when the particle swells and when an open heating process leads to increase loss of volatiles. It should be noted that a lower air/water partition coefficient results in a reduced loss of volatile, even if the molecules cross the water/air interface more quickly. Therefore, the air/water partition coefficient is the limiting factor in the loss of volatiles on cooking.

Discussion and Concluding Remarks

A mass transfer model was developed for estimation of the flavor release from particles, which either swell or erode in a solvent. The diffusion of water into the flavored particle is the key to flavor release from an immersed particle to air. This theoretical work has necessitated specifically designed experimental conditions to reduce considerably the number of variables and to check the model's validity.

For particles that swell, the water uptake rate and quantity are characteristics of the water diffusion coefficient function in the matrix polymer and of the phase volume of water present in the newly formed hydrogel.

Spin-echo NMR enables measurement of the water diffusion coefficient evolution with respect to the water-phase volume present in the matrix polymer.

Microscopy measurements were used to accurately estimate the water-phase volume necessary to develop hydrogel formation and water-phase volume present in the stable hydrogel. Reinjecting these parameters' values in the case of particles that erode enables shell thickness to be estimated before erosion.

UV spectroscopy measurements were used for determining the rate of molecule release from the particle to water and give good agreements between the model and experimental results and has been demonstrated under both swelling and erosion conditions.

Static headspace analysis was performed to characterize the transfer rate of flavor molecules through the water/air interface for different volatile species.

Finally, *dynamic headspace* analysis in specific experimental conditions demonstrates the validity of the theoretical work. This experiment intends to mimic real-life cooking where most of the volatile compounds are lost before consumption of the food. If the 15-min time difference between the closed and the opened experiment corresponds to the time of preparation of an instant soup in a pan on the stove, we clearly see the benefit of using a swelling particle. According to our model 80% of dimethyl sulfide would be lost in the air (68% experimentally) after 15 min in the case of eroding particles. When particles swell this loss is reduced to half: 40% (also in the experiment: 34%). Therefore our model predicts that a swelling particle would prolong the smell of a soup even after cooking and this has been confirmed by the headspace experiment.

Then it is possible to reduce the rate of flavor release by forcing a particle to swell. One way to obtain such behavior is to include HGP in the composition that will form a physical gel network at the periphery of the particle when immersed in water. According to the model developed here, the gel strength will indirectly play a minor role on controlling the flavor release in isothermal conditions because it will influence only the phase volume of water present in the gel (ϕ_1). The phase volume at the inner waterfront (ϕ_w) is independent of the presence of HGP (equivalent value for swelling and erosion). The HGP characteristics (such as nature, gel strength, backbone flexibility, number and nature of crosslinks, etc.) are expected to have an influence on ϕ_1. However, ϕ_1 is governed not only by the HGP networks characteristics, but also by the material released from the particle to the gel, including the nonvolatile molecules such as maltodextrin chains. Considering that the amount of HGP is small compared to the maltodextrin amount, we would not consider that ϕ_1 would evolve strongly for different HGP nature or concentration. The gels formed can have different properties and can promote stability in different conditions imposed by the application.

If the gel formed is stable at the application temperature, the flavor release is expected to follow similar kinetics.

Equation 7 is usually written taking into account the loss of gel molecules by slow polymer molecular diffusion induced by reptation. Increasing the HGP concentration can reduce the effect of this phenomenon by the formation of a denser gel network. Because the reptation is linked to the entropy of the gel, a rise in temperature would increase reptation and decrease gel stability. However, the HGP concentration must be low enough to preserve particle properties [that are, T_g, $D(\phi)$, etc.].

It has been demonstrated that the flavor release from encapsulated particles immersed in water is governed by the diffusion rate of water into the particle. We have compared the parameters of Eq. 5 obtained and published for different starch derivatives or sources, and it appears that modifying the carrier polymer modifies the swelling function. In the case of particle swelling, we believe that the flavor release is dominated by the nature of the polymer that forms the glassy matrix more than by the HGP composition or nature.

Acknowledgments

The authors gratefully acknowledge D. Ferdinando, Dr. D. Martin, and Dr. S. Ablett (Unilever Colworth Research, UK) and B. Ribot and Prof. A. Blake (Firmenich S.A. Geneva, Switzerland) for their invaluable input and fruitful discussions.

Literature Cited

Benczédi, D., "Flavour Encapsulation Using Polymer-Based Delivery Systems," *Food Flavour Technology*, A. J. Taylor, ed., Sheffield Academic Press, Sheffield, UK and CRC Press, Boca Raton, FL, pp. 153–166 (2002).

Benczédi, D., and P.-E. Bouquerand, "Process for the Preparation of Granules for the Controlled Release of Volatile Compounds," WO 01/17372 A1 (U.S. Patent No. 6 607 771) (2001).

Blake, A., and P. Attwool, "Particulate Flavor Compositions and Process to Prepare Same," U.S. Patent No. 5 786 017 (1998).

Callaghan, P. T., K. W. Jolley, and J. Lelièvre, "Diffusion of Water in the Endosperm Tissue of Wheat Grains as Studied by Pulsed Field Gradient Nuclear Magnetic Resonance," *Biophys. J.*, **28**, 133 (1979).

Coulson, J. M., and J. F. Richardson, *Chemical Engineering*, 3rd Edition, Volumes I, II, and III, Pergamon Press, Oxford, UK (1977).

Davey, M. J., K. A. Landman, M. J. McGuinness, and H. N. Jin, "Mathematical Modeling of Rice Cooking and Dissolution in Beer Production," *AIChE J.*, **48**, 1811 (2002).

Devotta, I., V. D. Ambeskar, A. B. Mandhare, and R. A. Mashelkar, "The Life Time of a Dissolving Polymeric Particle," *Chem. Eng. Sci.*, **49**, 645 (1994).

Eccles, C. D., P. T. Callaghan, and C. F. Jenner, "Measurement of the Self-Diffusion Coefficient of Water as a Function of Position in Wheat Grain Using Nuclear Magnetic Resonance," *Biophys. J.*, **53**, 77 (1988).

Fan, L. T., and S. K. Singh, *Controlled Release: A Quantitative Treatment. Polymer Properties and Applications*, Vol. 13, Springer-Verlag, Berlin (1989).

Gomi, Y. I., M. Fukuoka, T. Mihori, and H. Watanabe, "The Rate of Starch Gelatinization as Observed by PFG-NMR Measurement of Water Diffusivity in Rice Starch/Water Mixtures," *J. Food Eng.*, **36**, 359 (1998).

Landman, K. A., and C. P. Please, "Modelling Moisture Uptake in a Cereal Grain," *IMA J. Math Appl. Bus. Indus.*, **10**, 265 (1999).

Linforth, R. S. T., K. E. Ingham, and A. J. Taylor, "Time Course Profiling of Volatile Release from Foods during the Eating Process," *Flavour Science: Recent Developments*, A. J. Taylor and D. S. Mottram, eds., Royal Society of Chemistry, London, pp. 361–368 (1996).

Lopes Da Silva, J. A., S. M. Castro, and I. Delgadillo, "Effect of Gelatinisation and Starch Emulsifier Interactions on Aroma Release from Starch Rich Model Systems," *J. Agric. Food Chem.*, **50**, 1976 (2002).

Marin, M., I. Baek, and A. J. Taylor, "Flavor Release as a Unit Operation: A Mass Transfer Approach Based on a Dynamic Headspace Dilution Method," *ACS Symp. Ser.* (*Flavor Release*), **763**, 153 (2000).

McIver, R. C., F. Vlad, R. A. Golding, T. D. Leichssenring, and D. Benczédi, "Encapsulated Flavor and/or Fragrance Composition," Patent Application WO 02/065858 A1 (2002).

Mutka, J. R., R. C. McIver, C. A. Palmer, D. Benczédi, P. E. Bouquerand, and A. Firmenich, "Solid Delivery Systems for Aroma Ingredients," WO 00/25606 A1 (U.S. Patent No. 6 607 778) (2000).

Narasimhan, B., and N. A. Peppas, "The Role of Modeling Studies in the Development of Future Controlled-Release Devices," *Controlled Drug Delivery. Challenges and Strategies*, K. Park, ed., American Chemical Society, Washington DC, pp. 529–557 (1997).

Papanu, J. S., D. S. Soane, A. T. Bell, and D. W. Hess, "Transport Models for Swelling and Dissolution of Thin Films," *J. Appl. Polym. Sci.*, **38**, 859 (1989).

Parker, A., F. Vigouroux, and W. F. Reed, "Dissolution Kinetics of Polymer Powders," *AIChE J.*, **46**, 1290 (2000).

Peppas, N. A., J. C. Wu, and E. D. von Meerwall, "Mathematical Modeling and Experimental Characterization of Polymer Dissolution," *Macromolecules*, **27**, 5626 (1994).

Schultz, T. H., K. P. Dimick, and B. Mackover, "Incorporation of Natural Fruit Flavours into Fruit Juice Powders: I. Locking of Citrus Oil in Sucrose and Dextrose," *Food Technol.*, **Jan.**, 57 (1955).

Siepmann, J., H. Kranz, N. A. Peppas, and R. Bodmeier, "A New Model Elucidating the Transport Mechanisms and Predicting the Release Kinetics from HPMC Matrixes," Proc. of the 26th Int. Symp. Controlled Release Bioactive Materials, pp. 994–995 (1999).

Stapley, A. G. F., "Diffusion and Reaction in Wheat Grains," PhD Thesis, University of Cambridge, Cambridge, UK (1995).

Stapley, A. G. F., P. J. Fryer, and L. F. Gladden, "Diffusion and Reaction in Whole Wheat Grains during Boiling," *AIChE J.*, **44**, 1777 (1998).

Stapley, A. G. F., T. M. Hyde, L. F. Gladden, F. Lynn, and P. J. Fryer,

"NMR Imaging of the Wheat Grain Cooking Process," *Int. J. Food Sci. Technol.*, **32**, 355 (1997).
Suzuki, K., M. Aki, K. Kubota, and H. Hosaka, "Studies on the Cooking Rate Equations of Rice," *J. Food Sci.*, **42**, 1545 (1977).
Suzuki, K., K. Kubota, M. Omichi, and H. Hosaka, "Kinetic Studies on Cooking of Rice," *J. Food Sci.*, **41**, 1180 (1976).
Syarief, A. M., "A Study of Moisture Diffusion Coefficients for Yellow-Dent Corn Kernel (*Zea mays* L.)," PhD Thesis, University of Minnesota, Minneapolis (1984).
Takeuchi, S., M. Fukuoka, Y. Gomi, M. Maeda, and H. Watanabe, "An Application of Magnetic Resonance Imaging to a Real Time Measurement of the Change of Moisture Profile in a Rice Grain during Boiling," *J. Food Eng.*, **33**, 181 (1997a).
Takeuchi, S., M. Maeda, Y. Gomi, M. Fukuoka, and H. Watanabe, "The Change of Moisture Distribution in a Rice Grain during Boiling as Observed by NMR Imaging," *J. Food Eng.*, **33**, 281 (1997b).
Tanner, J. E., and E. O. Stejskal, "Restricted Self-Diffusion of Protons in Colloidal Systems by the Pulsed Gradient Spin Echo Method," *J. Chem. Phys.*, **49**, 1768 (1968).
Taylor, A. J., and R. S. T. Linforth, "Modelling Flavour Release through Quantitative Structure Property Relationships (QSPR)," *Chimia*, **55**, 448 (2001).
Thomas, N. L., and A. H. Windle, "A Theory of Case II Diffusion," *Polymer*, **23**, 529 (1982).

Manuscript received May 21, 2003, and revision received Mar. 23, 2004.